ELSEVIER

Materials Science and Engineering A 423 (2006) 19–23

MATERIALS SCIENCE & ENGINEERING A

www.elsevier.com/locate/msea

Load effects on the phase transformation of single-crystal silicon during nanoindentation tests

Jiwang Yan [a,*], Hirokazu Takahashi [b], Xiaohui Gai [c], Hirofumi Harada [d], Jun'ichi Tamaki [b], Tsunemoto Kuriyagawa [a]

[a] *Department of Nanomechanics, Tohoku University, Aramaki Aoba 6-6-01, Aoba-ku, Sendai 980-8579, Japan*
[b] *Department of Mechanical Engineering, Kitami Institute of Technology, Koen-cho 165, Kitami 090-8507, Japan*
[c] *Department of Material Science and Engineering, Tohoku University, Aobayama 02, Aoba-ku, Sendai 980-8579, Japan*
[d] *Siltronic Japan Corporation, 3434 Shimata, Hikari, Yamaguchi 743-0063, Japan*

Received 8 July 2005; received in revised form 2 September 2005; accepted 30 September 2005

Abstract

Depth-sensing nanoindentation tests were made on single-crystal silicon wafers at various loads using a sharp Berkovich indenter, and the resulting indents were studied using transmission electron microscope and selected area diffraction techniques. The results indicated that the shape of the unloading parts of the load–displacement curves was affected by indentation load. The geometry and the size of the phase transformation region were also dependent on the indentation load. A strong correlation between the indentation load and the microstructure change of silicon was confirmed. A small load (∼20 mN) leads to a complete amorphous indent after unloading, whereas a big load (∼50 mN) produces a mixture of amorphous and nano-crystalline structure around the indent. The critical load for this transition to occur was approximately 30 mN. These results provide information for ductile regime machining technologies of silicon parts.
© 2006 Elsevier B.V. All rights reserved.

Keywords: Nanoindentation; Silicon; Phase transformation; Amorphization; Microstructure change; Ductile regime machining

1. Introduction

Single-crystal silicon (Si) is the principal material used for solid-state electronics and infrared optical technologies. Over the recent decades, many stable and metastable solid phases of silicon have been observed in pure hydrostatic pressure tests and other deviatoric tests such as micro/nanoindentations. It has been shown that in indentation tests, a pressure-induced phase transformation occurs to silicon and the material directly underneath the indenter first transforms to a metallic state during loading; upon unloading, it transforms to an amorphous structure or other metastable phases [1–6]. The metallic phase having the β-tin structure is sufficiently ductile to sustain plastic flow, which provides the possibility of ductile regime machining of silicon parts [7].

Due to the fact that the mechanical contact conditions in an indentation test is geometrically akin to that in micro-nano level machining processes such as single-point diamond turning [7,8], the understanding of the indentation-induced deformation, fracture and microstructure change can provide useful information for improving the mechanical, optical and electronic performances of silicon products by eliminating the machining damages [9]. Previous workers have found that the phase transformation mechanisms during indentation tests depend on the indenter shape, loading/unloading rate and other factors [10–14]. These results are useful for the selection of machining conditions since the indenter shape corresponds to the tool geometry, and the loading/unloading rate corresponds to the machining speed in a machining process.

In the present paper, we explored the effect of the indentation load on the phase transformation of silicon. The indentation load corresponds to the machining scale, namely, the depth of cut or undeformed chip thickness, in machining processes. Previous authors have investigated the load effects during indentations with blunt spherical indenters [11–13]. In this paper, we used a sharp Berkovich indenter and examined the indents at various loads using a transmission electron microscope and selected area diffraction (SAD) techniques. The effects of maximum

* Corresponding author.
E-mail address: yanjw@pm.mech.tohoku.ac.jp (J. Yan).

0921-5093/$ – see front matter © 2006 Elsevier B.V. All rights reserved.
doi:10.1016/j.msea.2005.09.120

Downloaded from Yan Laboratory, Keio University at http://www.yan.mech.keio.ac.jp. Redistribution is subject to copyright licence from the journal publisher.

indentation load on the loading–unloading characteristics, the depth of the phase transformation region and the microstructure change of silicon were examined.

2. Experimental

Indenter shape has a strong effect on the indentation behavior. Usually, pyramidal indenters such as Vickers, Berkovich and Knoop indenters are typically classified as sharp, whereas spherical indenters are characterized as blunt. To simulate an ultraprecision machining process a sharp indenter is much more suitable than a blunt one, due to the fact that in ultraprecision machining processes, extremely sharp tools are always used.

A nanoindentation tester, ENT-1100a, produced by Elionix Co. Ltd., was used for the experiments. Tests were performed using a Berkovich indenter made of single crystalline diamond. The tip radius of the indenter was estimated to be ∼20 nm. The circumferential orientation of the silicon wafer to the indenter was adjusted to make the orientation flat [1 1 0] parallel to one face of the indenter. The maximum load was varied in the range of 1–200 mN. The time for loading and unloading was the same and fixed to 5 s; thus, the loading/unloading rate changed in the range of 0.2–40 mN/s. Ten indentation tests were made for each experimental condition.

Device grade p-type single-crystal silicon wafers having a doping level of 1.33×10^{14} atoms/cm^3 were used as specimens. The surface orientation of these silicon wafers is (0 0 1). These wafers are 0.725 mm in thickness and obtained with chemomechanical polished finishes. Thin-foil specimens for cross-sectional transmission electron microscopy (XTEM) were prepared using a focus ion beam (FIB) apparatus in such a way that the specimen contains the loading direction and the center of the indent. These specimens were then examined using a high resolution TEM (HRTEM), Hitachi H-9000NAR, at an accelerating voltage of 300 kV. The maximum direct magnification was 400,000 times and an extension magnification of 5 times was used, leading to a total magnification of 2,000,000 times.

3. Results

3.1. Load–displacement characteristics

The load–displacement curves of silicon indentation tests have been the main interest for previous studies [10,12]. Some observed a distinct displacement discontinuity in loading, called pop-in; but others additionally recorded well-defined transition steps only in unloading, called pop-out. These features on the loading–unloading curves are considered to be related to the density change of silicon caused by the high pressure phase transformations. In loading, diamond cubic silicon transforms to the denser phase and thus the pop-in appears due to a sudden volumetric reduction. In contrast, in unloading the transition is to a lower density structure associated with a volumetric expansion, and consequently the pop-out occurs. Moreover, these features on the loading–unloading curves were also found to be dependant on the indenter geometry and loading/unloading rates [10,14].

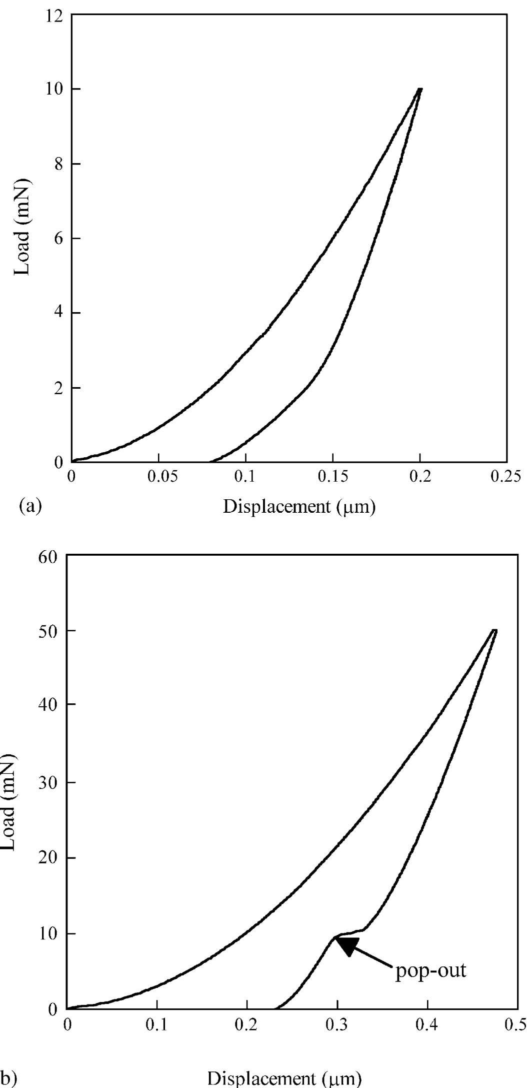

Fig. 1. Typical load–displacement curves during the indentations at various loads: (a) 10 mN and (b) 50 mN, showing different features on the unloading part.

In the present experiments, when the maximum load was varied in the range of 1–200 mN, no pop-in events were found for all the conditions. However, apparent different features were confirmed on the unloading curves for various loads. Typical load–displacement curves are shown in Fig. 1. When the maximum indentation load was 10 mN, a slight elbow (gradual change in slop) can be seen on the unloading part of the curves, as in Fig. 1(a). This is similar to previous results under fast unloading conditions, indicating a transformation from diamond cubic structure to amorphous [10]. In contrast, at the maximum indentation load of 50 mN, a well-defined pop-out appeared on the unloading part of the curve, as shown in Fig. 1(b). The critical load for the occurrence of pop-out was found to around 30 mN. These results imply the possible differences in phase transformation mechanism under various indentation loads even for the same indenter shape.

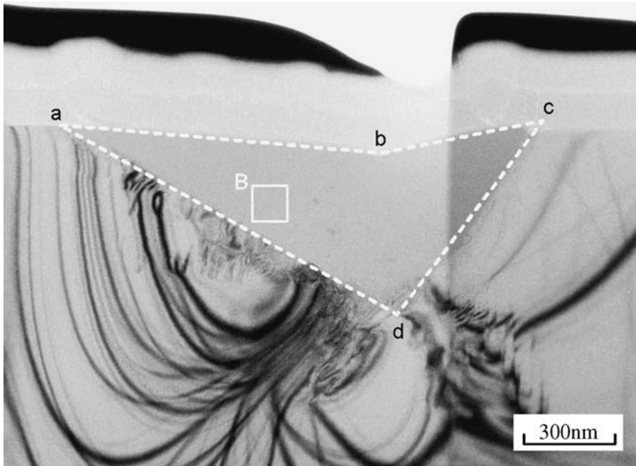

Fig. 2. Cross-sectional TEM image of an indent obtained at a load of 20 mN.

3.2. XTEM observation

Fig. 2 is a bright field XTEM micrograph of an indent made at a maximum load of 20 mN. The dotted line *abc* shows the indent surface after unloading. Just below the indent surface, a light grey region indicated by *abcd* can be identified. The material within the region *abcd* has a uniform microstructure and there can be seen a clear boundary between this region and its surrounding area. This region, as known from the high resolution observation results in Fig. 5 which will be shown later, is a phase transformation region. The depth of the phase transformation region (655 nm) is approximately 4.8 times that of the residual depth of the indent (136 nm), and 2.3 times the maximum indentation depth (280 nm) identified from the corresponding load–displacement curve. The long stripes shown out of the *abcd* region are interference fringes caused by the bending of the TEM sample due to FIB processing.

Fig. 3 is an XTEM micrograph of an indent made at a maximum load of 50 mN. Similarly to Fig. 2, a phase transformation region indicated by dotted line *abcd* can be identified. However, what to note is that the microstructure of the phase transformation region is distinctly different from that shown in Fig. 2. Numerous dark spots can be observed in the central lower region of the indent, though the upper regions on the two sides were similar to the phase transformation region in Fig. 2. The depth of the phase transformation region in Fig. 3 is approximately 1036 nm, 3.8 times that of the residual depth of the indent (273 nm) and 2.2 times the maximum indentation depth (475 nm).

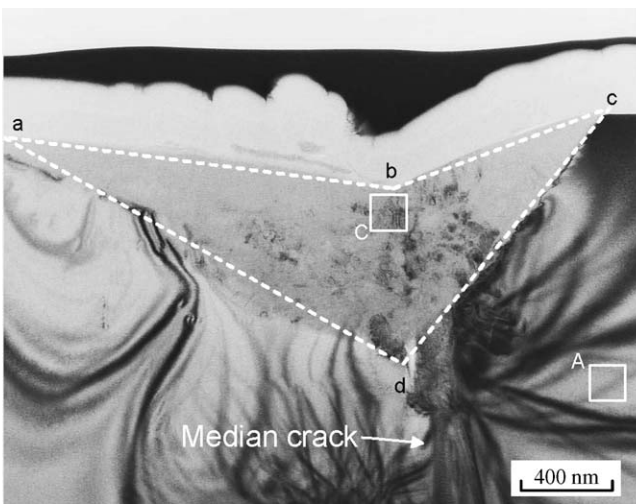

Fig. 3. Cross-sectional TEM image of an indent obtained at a load of 50 mN.

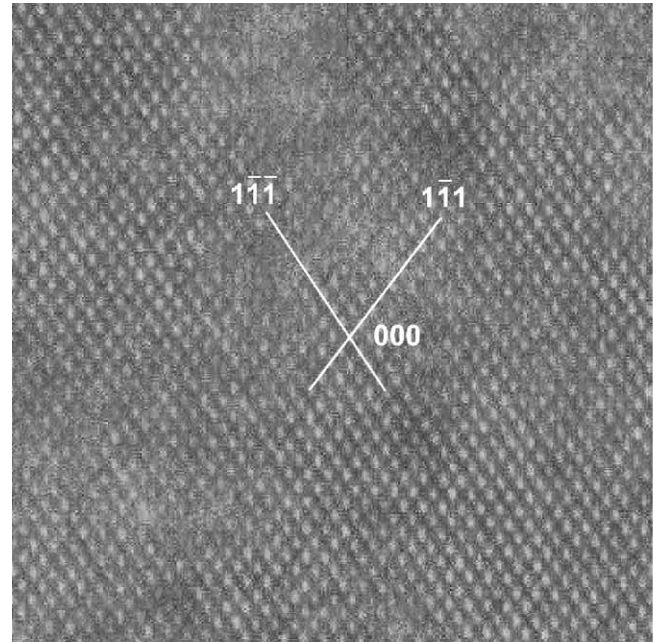

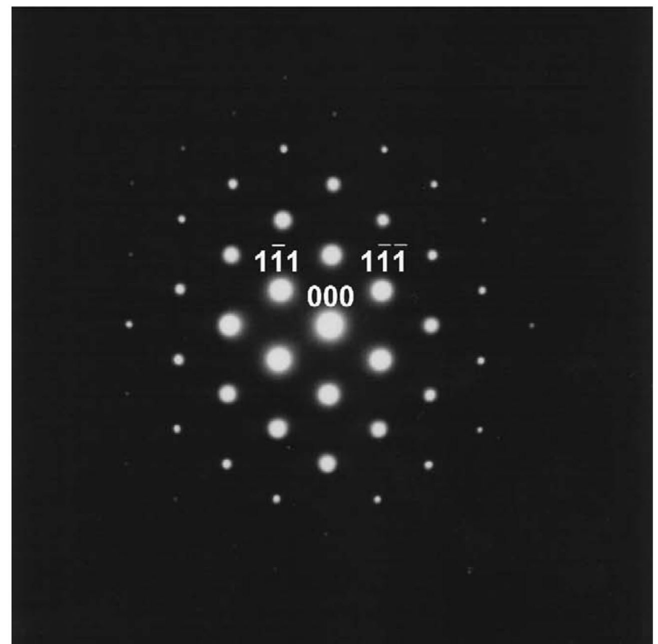

Fig. 4. HRTEM image (a) and SAD pattern (b) of the region indicated by square A in Fig. 3.

The results in Figs. 2 and 3 indicate that as the maximum load increases, the ratio of the phase transformation region depth to the maximum indentation depth maintains constant; while the ratio of the phase transformation region depth to the residual indent depth decreases. In other words, the phase transformation mechanism during loading is independent of the maximum load; while during unloading, the phase transformation mechanism is maximum load dependent. Therefore, the results demonstrate that different metastable phases of silicon were generated during unloading at various maximum loads. Furthermore, it is also assumable that the metastable phase generated at a maximum load of 50 mN has much higher density than the amorphous phase produced at 20 mN.

Another thing to note in Fig. 3 is that a median crack is extending downward from the bottom of the phase transformation region, which indicates that the critical load for micro-fracture initiation has been exceeded. This situation corresponds to the size effect of the ductile–brittle transition of a machining process [8].

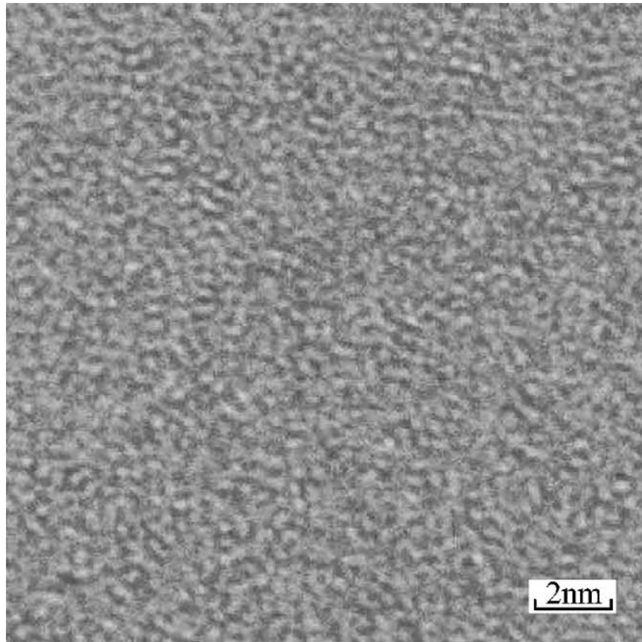

(a)

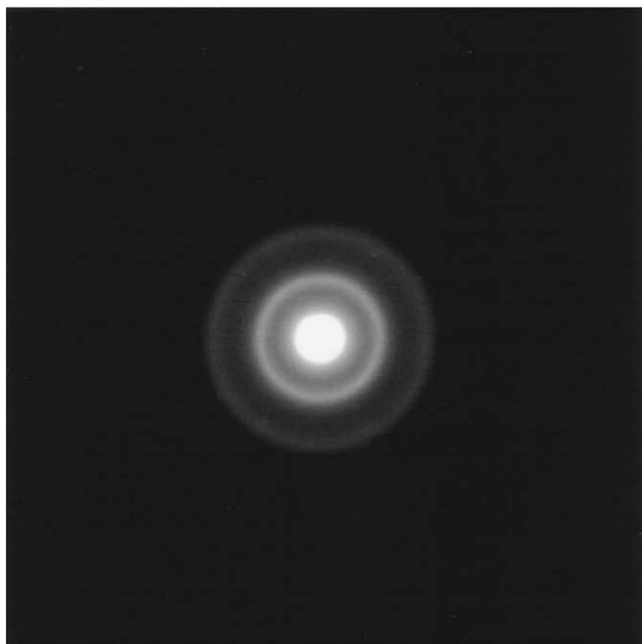

(b)

Fig. 5. HRTEM image (a) and SAD pattern (b) of the region indicated by square B in Fig. 2.

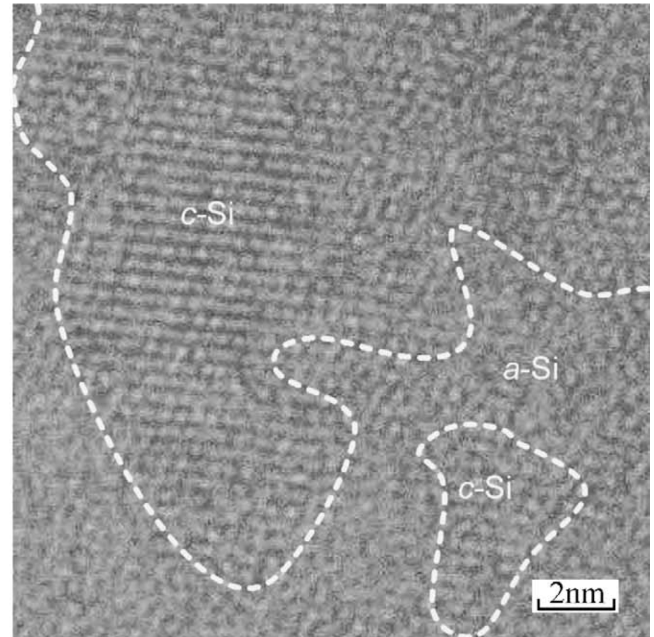

(a)

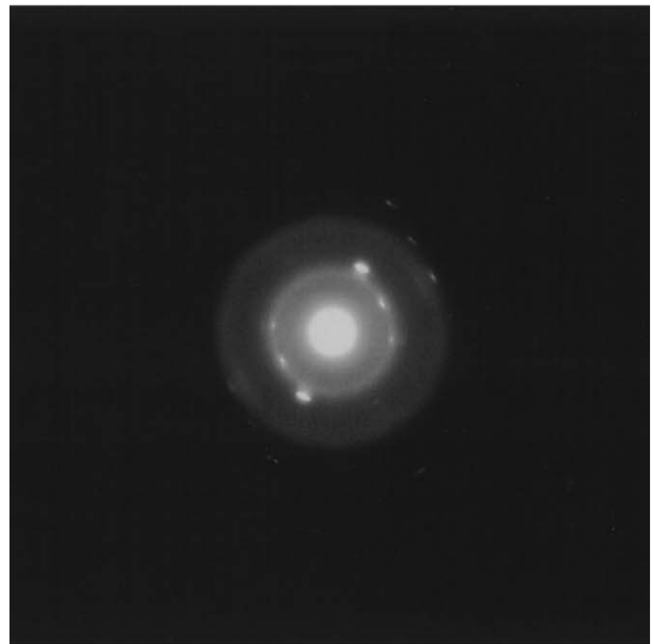

(b)

Fig. 6. HRTEM image (a) and SAD pattern (b) of the region indicated by square C in Fig. 3.

3.3. HRTEM and SAD analysis

Fig. 4 is the HRTEM image and SAD pattern of the region marked by square A in Fig. 3, which is located outside the indent. In Fig. 4(a), silicon atoms are arranged in regular lattice structures, and only diffraction spots of [1 1 0] incidence can be seen in Fig. 4(b). These results indicate a perfect diamond cubic single-crystalline structure without any phase transformation and damages.

Fig. 5 is the results of the region indicated by square B in Fig. 2, which is located inside the indent obtained at the maximum load of 20 mN. In Fig. 5(a), silicon atoms are distributed randomly, without any visible lattice structure. In Fig. 5(b), only halo rings can be seen, indicating a complete amorphous state.

Fig. 6 shows the results of the region marked by square C in Fig. 3, which is located inside the indent at the maximum load of 50 mN. As enclosed by dotted lines in Fig. 6(a), extremely small crystalline grains (c-Si) of nanolevel size are surrounded by the amorphous phase (a-Si). The nano-crystalline grains are irregular in shape and size. The lattice orientations of these grains were different from the diamond cubic substrate, indicating that the nano-crystalline grains have been rotated within amorphous phase due to the indentation deformation. In Fig. 6(b), both halo rings and diffraction spots can be confirmed, which also indicates a mixture of amorphous state and crystalline state.

4. Discussion

It has been known from previous works that during unloading of an indenter, the β-tin silicon transforms through the metastable silicon (R8) to body-centered cubic (bcc), or directly to amorphous silicon, depending on the unloading rates [12]. The results from this study revealed that the phase transformation mechanism also depends on the maximum load. This effect might be due to the changes in the hydrostatic pressure and/or the deviatoric shearing stress/strain conditions under various maximum loads. The load-effect has also been found in ductile machining processes as size-effects. One of the present authors (J.Y.) examined the single-pointed diamond machined silicon substrates using laser micro-Raman and found that the extent of subsurface amorphization in diamond turning depends significantly on the undeformed chip thickness [15]. An extremely small undeformed chip thickness leads to ductile regime machining and causing an amorphous subsurface layer; whereas a large undeformed chip thickness causes brittle regime machining and causes a damaged subsurface layer containing crystalline phase. The trend in machining was well consistent with the load effects in indentation tests reported in this paper.

5. Conclusions

Nanoindentation tests were made on single-crystal silicon wafers at various loads using a Berkovich indenter, and the indents were studied using TEM and SAD techniques. The material beneath the indenter undergoes phase transformation after unloading, and the microstructure change mechanism depends on the maximum indentation load. An extremely small indentation load (∼20 mN) leads to a complete amorphous region, whereas a big load (∼50 mN) gives rise to a mixture of amorphous and nano-crystalline structure. The depth of the phase transition region is a few times that of the residual indent depth, and their ratio decreases as the maximum indentation load increases. A median crack was found to be initiated earlier than any other types of cracks under a load of 50 mN. The results from this paper also confirmed that the load-dependent nature of the unloading curves, namely pop-out events, is related to the different phase transformation mechanisms at various indentation loads.

References

[1] D.R. Clarke, M.C. Kroll, P.D. Kirchner, R.F. Cook, Phys. Rev. Lett. 60 (1988) 2156–2159.
[2] G.M. Pharr, W.C. Oliver, D.S. Harding, J. Mater. Res. 6 (1991) 1129–1130.
[3] D.L. Callahan, J.C. Morris, J. Mater. Res. 7 (1992) 1614–1617.
[4] A. Kailer, Y.G. Gogotsi, K.G. Nickel, J. Appl. Phys. 81 (1997) 3057–3063.
[5] Y. Gogotsi, C. Baek, F. Kirscht, Semicond. Sci. Technol. 14 (1999) 936–944.
[6] J.E. Bradby, J.S. Williams, M.V. Swain, Phys. Rev. B 67 (2003) 085205.
[7] J. Yan, M. Yoshino, T. Kuriyagawa, T. Shirakashi, K. Syoji, R. Komanduri, Mater. Sci. Eng. A 297 (2001) 230–234.
[8] J. Yan, K. Syoji, T. Kuriyagawa, H. Suzuki, J. Mater. Process. Tech. 121 (2002) 363–372.
[9] J. Yan, H. Takahashi, J. Tamaki, X. Gai, H. Harada, J. Patten, Appl. Phys. Lett. 86 (2005) 181913.
[10] V. Domnich, Y. Gogotsi, S. Dub, Appl. Phys. Lett. 76 (2000) 2214–2216.
[11] L. Zhang, I. Zarudi, Int. J. Mech. Sci. 43 (2001) 1985–1996.
[12] H. Saka, A. Shimatani, M. Sugamura, Suprijadi, Philos. Mag. A 82 (2002) 1971–1981.
[13] I. Zarudi, J. Zou, L.C. Zhang, Appl. Phys. Lett. 82 (2003) 874–876.
[14] J. Jang, M.J. Lance, S. Wen, T.Y. Tsui, G.M. Pharr, Acta Mater. 53 (2005) 1759–1770.
[15] J. Yan, J. Appl. Phys. 95 (2004) 2094–2101.